



OPEN Spatial risk patches of the Indian crested porcupine crop damage in southeastern Iran

Kamran Almasieh¹✉ & Alireza Mohammadi²

Human-wildlife conflict (HWC) represent a significant global issue, leading to economic losses for humans due to the destruction of agricultural products and livestock. This study was conducted in southeastern Iran with two primary objectives: to identify the major environmental variables influencing spatial risk modeling and to pinpoint spatial risk patches and hotspots of agricultural damage caused by the Indian crested porcupine (ICP) in this region. An ensemble modeling technique was used to evaluate the spatial risk of agricultural damage caused by the ICP, drawing on 111 independent conflict records and nine environmental factors. The findings indicated that the distance to villages, orchard density, cropland density, and Normalized Difference Vegetation Index emerged as the most significant variables in modeling the spatial risk of crop damage from the ICP in the study region. Nine spatial risk patches, comprising approximately 8% of the study area, were identified for crop damage attributed to the ICP. The three largest spatial risk patches, located in the west of the study area, accounted for 80% of all predicted crop damage patches caused by the ICP. Additionally, hotspots of agricultural damage were clustered in the western part of the study area. Conservation areas covered about 8% of the predicted spatial risk patches and 2.4% of the hotspots of agricultural damage, respectively. Urgent attention is needed to reduce human-ICP conflicts in the identified risk patches. We strongly recommend implementing fencing around cultivated lands and individual tree trunks, as well as enhancing local knowledge and insurance for agricultural products, to mitigate human-ICP conflicts in the study area.

Keywords Crop damage, Spatial risk modeling, Human-wildlife conflicts, Indian crested Porcupine, Iran

The ever-increasing expansion of human activities and the encroachment of human infrastructure on natural landscapes have led to a rise in human-wildlife conflicts (HWC)^{1,2}. HWC is a global issue that results in significant economic damage to humans due to the destruction of agricultural products and losses in livestock^{3–5}. In addition, residents employ various methods to prevent damage or retaliation against local species, such as trapping and shooting, to eliminate these species⁶. The escalating conflict undermines local cooperation for species conservation, jeopardizing the long-term survival of wildlife due to retaliatory killings^{7,8}. Previous studies on HWC have primarily concentrated on large carnivores^{9–12}. However, mammals that are considered pests of agricultural products can inflict significant damage to these resources^{5,13}.

The Indian crested porcupine (*Hystrix indica* Kerr, 1792), hereafter referred to as ICP, is a large Asiatic rodent recognized for its long quills. This species is found in 19 countries, ranging from the eastern Mediterranean to Southwest and Central Asia (Supplementary Information: Fig. S1). Due to its wide distribution, the ICP is categorized as Least Concern (LC) by the IUCN Red List¹⁴. However, the ICP faces threats from overharvesting in Southwest Asia¹⁵. Consequently, this species is considered vulnerable in Jordan, near threatened in Turkey, and threatened in Iraq^{15–17}. The ICP is a strictly nocturnal and generalist herbivore that spends the daytime in dens. It feeds on a variety of natural geophytes and hemi-cryptophyte species, as well as grains, fruits, and the bark of trees⁷. The ICP digs into the ground to consume plant roots, and the burrows created by this species are clearly visible¹⁸. This species have been identified as an apex ecosystem engineers by providing crucial ecological niche for various other co-occur animals¹⁹. However, The ICP has been identified as a species in conflict with humans in various regions of Asia⁷. In western Asia, the ICP is threatened and is considered an agricultural pest due to its tendency to raid crops and debark the trees of orchards at ground level¹⁵. For example, in Pakistan, the ICP causing widespread crop damage and prompting various human responses. The most affected crop by

¹Department of Nature Engineering, Agricultural Sciences and Natural Resources University of Khuzestan, Mollasani, Iran. ²Department of Environment Science and Engineering, Faculty of Natural Resources, University of Jiroft, Jiroft, Iran. ✉email: almasieh@asnruk.ac.ir

the ICP is maize followed by other crops such as potatoes, tomatoes, and various greens^{20,21}. Economic losses are substantial, with many farmers reporting annual losses ranging from \$101 to \$300 due to ICP damage²¹. The damage poses a threat to food security and subsistence farming, particularly in regions where agriculture is the primary livelihood source. While specific cultural disruptions are not extensively documented, the reliance on agriculture for sustenance suggests that crop losses could indirectly affect cultural practices tied to farming cycles and community gatherings around harvests. Farmers use a mix of strategies to mitigate porcupine damage such as lethal control and hunting. ICPs are also hunted for medicinal purposes and as a food source²². While hunting occurs, there is limited research on its long-term effects on ICP populations. Relocation is rarely mentioned as a viable option, indicating a preference for immediate lethal control²³. The ICP is the largest rodent in Iran, with a vast distribution²⁴. The Persian leopard (*Panthera pardus tulliana*) is the natural predator of the ICP. In areas where the leopard population is locally extinct or significantly reduced, the ICP has become a pest, damaging agricultural crops, trees in orchards, and, in some cases, natural woodlands²⁵. In certain regions of Iran, they are hunted and consumed for their meat for medical reasons, such as the treatment of respiratory diseases like asthma, which has contributed to a decline in the species' population¹⁸.

It is essential to identify areas with a high risk of large rodents damaging crops in order to protect these species²⁶. Spatial risk models used to predict areas at high risk for crop damage caused by large rodents, analyze the relationship between environmental variables and agricultural damage to identify landscapes associated with a heightened risk of damage²⁷. These models can effectively detect areas with a high probability of HWC due to the non-random distribution patterns of such conflicts²⁸. Spatial risk patches, defined in this paper as areas with a high likelihood of conflict due to large rodents, should be prioritized for mitigating HWC²⁹. Recognizing key factors in spatial risk modeling is vital for safeguarding species in regions susceptible to significant crop damage caused by large rodents⁴. Furthermore, areas with a higher frequency of damage reports, and thus an increased likelihood of conflict, have been identified as hotspots^{30,31}.

Locals in rural areas who rely on agricultural livelihoods typically have low incomes compared to their urban counterparts. Consequently, damage to agricultural products can lead to significant social and economic repercussions for these communities³². Conversely, minimizing human-ICP conflict is crucial for the survival of species in human-occupied landscapes³³. Crop raiding by ICPs is particularly prevalent in the arid and semi-arid regions of southeastern Iran. As a result, this species is often identified as a source of conflict for local farmers. Therefore, this study was conducted in southeastern Iran with two primary objectives: (1) to identify the key environmental variables involved in spatial risk modeling and (2) to pinpoint spatial risk patches and hotspots of agricultural damage caused by the ICP within the region. Our findings offer insights into how human-ICP conflict can be mitigated by illustrating the environmental preferences of this species in southeastern Iran, where crop-raiding incidents are most prevalent.

Materials and methods

Study area

The study area encompasses three provinces: Sistan and Baluchistan, Hormozgan, and Kerman, located in the southeast of Iran (Fig. 1). This region covers approximately 433,000 km², accounting for 26.3% of Iran's total area. Two distinct climatic and topographic zones are present within the study area. The first zone includes Sistan and Baluchistan, Hormozgan, and southern Kerman, characterized by vast arid plains, hot summers, mild winters, and annual precipitation ranging from 100 to 150 mm. The primary natural tree species in the sparse woodlands of this area include *Tamarix* spp., *Nannorrhops ritchiana*, and *Prosopis cineraria*³⁴. Additionally, *Phoenix dactylifera* is the predominant tree found in the orchards of these provinces. The impact of damage to these trees, as observed in some cases by the ICP, exacerbates the human-ICP conflict in these regions (Fig. S2). North of Kerman lies a distinct mountainous region characterized by milder summers, colder winters, and an annual precipitation of 350 mm. The primary native tree species in this area include *Pistacia khinjuk*, *P. atlantica*, and *Amygdalus lycioides*³⁴. Locals utilize the fruit and gum from these trees, particularly *P. atlantica*; however, the local economy suffers due to the drying of these trees caused by the bark stripping inflicted by the ICP. Additionally, various tree species, such as *Juglans* spp. and *Ficus carica*, are found in the orchards of this region, which are also adversely affected by ICP as it debarks the trees at ground level. Furthermore, ICP has caused significant damage to agricultural crops, especially *Medicago sativa* and *Vicia faba*. Locals have also reported damage to irrigation tubes. Approximately 12.4% of the study area is designated as conservation areas (CAs) (Fig. 1).

Conflict records and environmental variables

In the study area, rangers and experts from the Department of Environment (DoE) provincial offices recorded a total of 124 instances of agricultural damage linked to the ICP (conflict records) across the three provinces of Sistan and Baluchistan, Hormozgan, and Kerman between the years 2015 and 2023. These records are considered reliable, as rangers and experts conducted site visits following each report of agricultural damage. During these visits, they identified the responsible species by examining the effects of the damage and looking for signs such as quills, footprints, and scat at the damage site, as well as interviewing witnesses. To minimize spatial-autocorrelation, based on the maximum home range of the ICP, which is 8 km²²², a 2 km radius was applied around each conflict record for spatial filtering. This was done using the Spatially Rarefy Occurrence Data tool within the SDMtoolbox³⁵. This radius is twice the amount considered for reducing the density of the occurrence points of the crested porcupine (*Hystrix cristata*) in Italy⁵. Thirteen conflict records were excluded, resulting in 111 independent records used for spatial risk modeling (Fig. 1).

All pertinent environmental variables ($n = 30$), encompassing human-related factors, land cover, water resources, protection measures, topography, and climate conditions, were primarily taken into account to model the spatial risk areas of agricultural damage resulting from ICP (see Table 1). Human-wildlife conflict is influenced

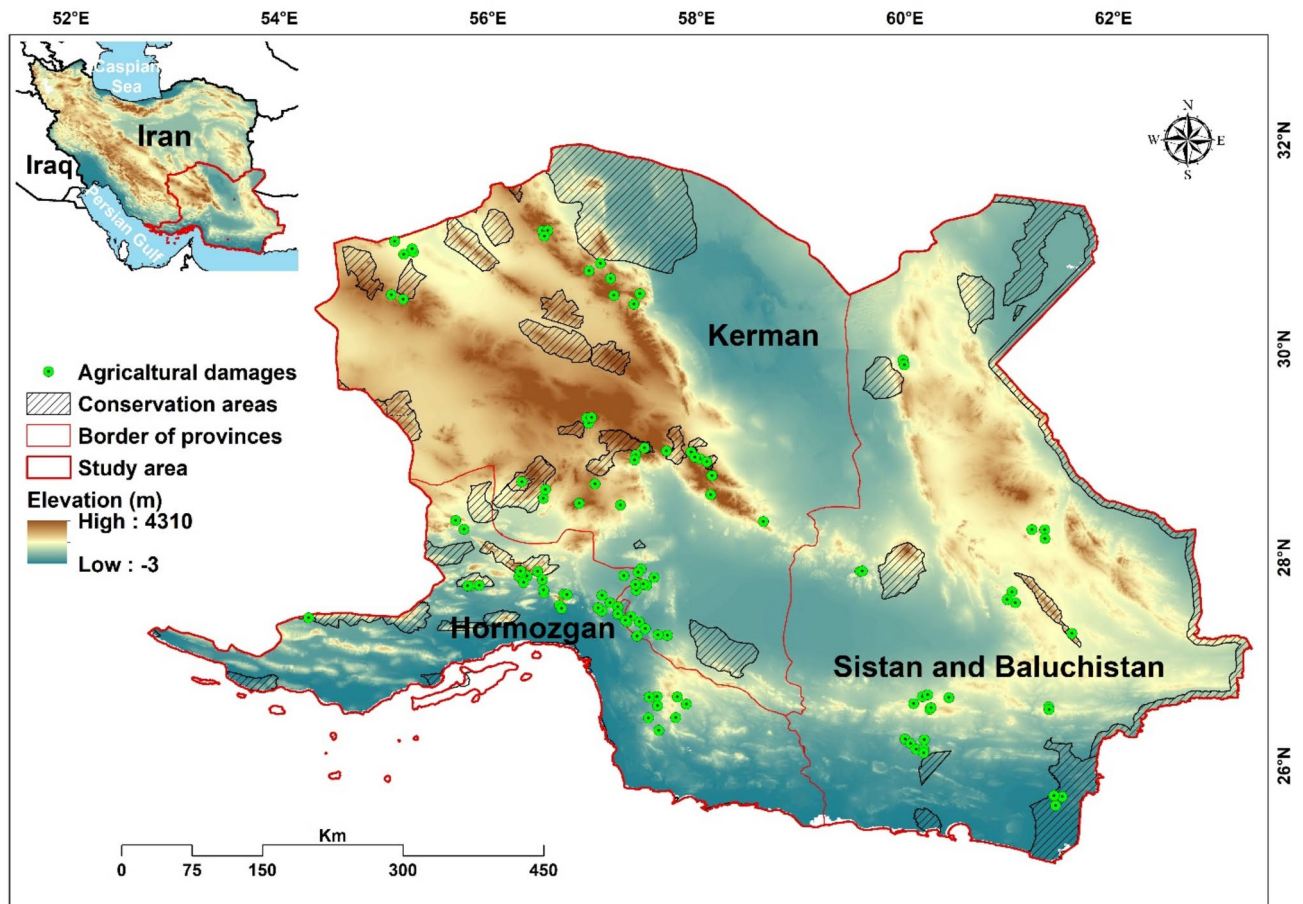


Fig. 1. Study area with two distinct topographic zones encompassing the three provinces of Sistan and Baluchistan, Kerman, and Hormozgan in southeastern Iran, highlighting the locations of agricultural damage caused by the Indian crested porcupine. ArcGIS software version 10.1 (<https://www.esri.com/en-us/arcgis/products/arcgis-pro/resources>) was used to generate the figure.

by population density, as well as the closeness to human settlements and other man-made structures²⁸. Therefore, distances to villages and roads were established as human-related variables using the Euclidean distance tool. We employed Inverse Distance Weighting (IDW) to create a variable representing human population density by interpolating the population density of villages²⁸. The human footprint, as discussed by Venter et al.³⁶, is another variable associated with human activity that serves as an indicator of human access, infrastructure, and population density with a base resolution of 1 km³⁷. Due to agricultural damages by the ICP¹⁵, the orchards (woody production) density and croplands (cultivated fields with herbaceous production) density were derived from the land cover map of Iran. A circular moving window with a five-kilometer radius was employed to generate density maps for these land cover types³⁸. The Normalized Difference Vegetation Index (NDVI) was calculated using 16-day composite MODIS data (MODIS MYD 13 A1 V6 map at a 500-meter resolution; <http://earthexplorer.usgs.gov>), based on the average values for the year 2023. Additionally, the distance to rivers was used as the water source for the species. The distance to CAs was considered a protective factor for the ICP. Topographic factors are dominant variables to predict distribution of species²⁸. A Digital Elevation Model (DEM) was sourced from <http://srtm.csi.cgiar.org>, featuring a resolution of 250 m. This data originated from the 90-meter Shuttle Radar Topography Mission (SRTM, <http://earthexplorer.usgs.gov>). The DEM was utilized to generate a slope variable. Climate determine the distribution of porcupines³⁹. Therefore, nineteen bioclimatic variables were analyzed, comprising eleven temperature variables and eight precipitation variables with a base resolution of 1 km⁴⁰ (<http://worldclim.org>). All variables were resampled to a resolution of 1 km. In ArcGIS version 10.1⁴¹ (<https://www.esri.com/en-us/arcgis/products/arcgis-pro/resources>), all the tools necessary for creating variables are accessible.

To select the final variables for spatial risk modeling, the R package MaxentVariableSelection^{42,43} was utilized, with an inter-correlation threshold set at 0.7, a regularization multiplier ranging from 1 to 5 in increments of 0.5, and a contribution threshold of 5%. The variables were chosen based on the lowest Akaike Information Criterion (AIC) and the highest Area Under the Curve (AUC) of the Receiver Operating Characteristic (ROC). Additionally, to exclude previously selected variables with a Variance Inflation Factor (VIF) of less than 3⁴⁴, the VIF of the dataset was assessed using the R package USD⁴⁵ (see Table 1).

| Variable categories | Variables (unit in parenthesis) | Selected by MaxentVariableSelection | VIF value | Final selection |
|---------------------|--|-------------------------------------|-----------|-----------------|
| Human | Distance to villages (degrees) | * | 1.13 | * |
| | Distance to roads (degrees) | * | 1.43 | * |
| | Population density of villages (person/km ²) | * | 1.35 | * |
| | Human footprint | | | |
| Land-cover | Orchards density (0–1) | * | 1.27 | * |
| | Croplands density (0–1) | * | 1.36 | * |
| | NDVI (–1–1) | * | 1.19 | * |
| Water | Distance to rivers (degrees) | | | |
| Protection | Distance to CAs (degrees) | * | 1.18 | * |
| Topography | Elevation (meter) | | | |
| | Slope (degrees) | | | |
| Climate | Annual mean temperature (BIO1) (°C) | | | |
| | Mean diurnal range (BIO2) (°C) | | | |
| | Isothermality (BIO3) (%) | | | |
| | Temperature seasonality (BIO4) (%) | | | |
| | Max temperature of warmest month (BIO5) (°C) | | | |
| | Min temperature of coldest month (BIO6) (°C) | | | |
| | Temperature annual range (BIO7) (°C) | | | |
| | Mean temperature of wettest quarter (BIO8) (°C) | | | |
| | Mean temperature of driest quarter (BIO9) (°C) | * | 1.67 | * |
| | Mean temperature of warmest quarter (BIO10) (°C) | | | |
| | Mean temperature of coldest quarter (BIO11) (°C) | | | |
| | Annual precipitation (BIO12) (mm) | | | |
| | Precipitation of wettest month (BIO13) (mm) | | | |
| | Precipitation of driest month (BIO14) (mm) | * | 1.58 | * |
| | Precipitation seasonality (BIO15) (%) | | | |
| | Precipitation of wettest quarter (BIO16) (mm) | | | |
| | Precipitation of driest quarter (BIO17) (mm) | | | |
| | Precipitation of warmest quarter (BIO18) (mm) | | | |
| | Precipitation of coldest quarter (BIO19) (mm) | | | |

Table 1. Environmental variables utilized in spatial risk modeling of agricultural damage caused by the Indian crested porcupine within the study area in southeastern Iran.

Spatial risk modeling

Spatial risk modeling of agricultural damage caused by the ICP in the study area was performed using the R package *Biomod2*⁴⁶. *Biomod2* identifies regions with consistent predictions by integrating multiple models, allowing for a comprehensive assessment of predictions with high reliability^{2,47}. As a result, ensemble modeling improves prediction accuracy by combining various models instead of depending on a single uncertain forecast^{47–50}. Five prediction models were employed for spatial risk modeling, including two regression-based models: the Generalized Linear Model (GLM) and Multivariate Adaptive Regression Splines (MARS), as well as three machine-learning models: Maximum Entropy (MaxEnt), Generalized Boosting Model (GBM), and Random Forest (RF). The performance of these models was evaluated using the AUC and the True Skill Statistic (TSS)⁵¹. To facilitate this assessment, five hundred pseudo-absence points were randomly created throughout the study area, ensuring they were located outside a 2 km radius from each agricultural damage point⁵². 75% of the agricultural damage points identified by the ICP were designated as the training dataset, while the remaining 25% served as the test dataset. For enhanced reliability, analyses were conducted with 20 replicates at a prevalence of 0.5, meaning that agricultural damage points and pseudo-absence points were given equal weights^{53,54}. The average contributions of variables from five models for risk assessment were computed using *Biomod2*. Furthermore, the response curves illustrating how agricultural damage points reacted to variables in the most accurate model were presented for the study area. The continuous ensemble spatial risk map was transformed into a binary map by applying the 10 th percentile of higher risk value at the conflict records within the ICP dataset⁵⁵. Patches containing agricultural damage points identified by the ICP were classified as spatial risk patches, while very small risk patches (less than 8 km²) were excluded from consideration. The conversion to a binary map and the creation of patches were accomplished using ArcGIS.

Hotspots of Indian crested porcupine crop damage

The Optimized Hot Spot Analysis tool in ArcGIS was employed to detect areas of significant crop damage attributed to the ICP. A grid with dimensions of 1.5 × 1.5 km² was utilized to divide the study area, allowing for the counting of damage records ($n = 111$) within each grid cell. The Getis–Ord Gi* statistic was computed

based on the geographic coordinates of the damage records located in each cell^{30,31}. This statistic is derived from a z-score, which reflects the distance between cells and the number of damage incidents recorded in each cell. Cells that exhibited a high frequency of damage records were assigned higher scores and identified as hotspots³⁰.

Results

Ensemble modeling and variable contribution

MaxentVariableSelection identified nine environmental variables for spatial risk modeling that exhibited the lowest Akaike and the highest AUC. VIF analysis did not exclude any of these nine variables (see Table 1). In the Biomod2 analyses, all models demonstrated excellent performance, with AUC and True Skill Statistic (TSS) values exceeding 0.9 and 0.75, respectively, with the Generalized Boosted Model (GBM) achieving the highest scores (refer to Supplementary Information: Table S1). According to the average contributions of the variables across five models, the key factors affecting spatial risk modeling of agricultural damage from the ICP in the study area were identified as distance to villages, orchard density, cropland density, and NDVI (see Table 2).

As the distance from villages increased, the probability of agricultural damage declined sharply before stabilizing at approximately 1 km. In contrast, the probability of agricultural damage rose as the distance from roads increased, eventually stabilizing at around 4 km. A higher human population density was associated with a gradual increase in the likelihood of agricultural damage, which leveled off at approximately 17,000 people per km² (Fig. 2). Similarly, greater densities of orchards and croplands led to a notable rise in the probability of agricultural damage. An increase in NDVI values also corresponded to a higher likelihood of agricultural damage, stabilizing at 0.15 on a scale ranging from -1 to 1. Conversely, the probability of agricultural damage decreased as the distance from CAs increased, stabilizing at a distance of 8 km (Fig. 2). Furthermore, as the mean temperature during the driest season dropped from 33 °C to 25 °C, there was a sharp decline in the likelihood of agricultural damage. A similar trend was observed with precipitation levels during this season; as they rose from 2 mm to 8 mm, the probability of agricultural damage steadily decreased.

The ensemble spatial risk map revealed that the west regions of the study area had the highest probabilities of agricultural damage due to the effects of the ICP. Furthermore, several isolated high-risk areas were identified in the eastern and southeastern parts of the study area (refer to Fig. 3). The spatial risk models from five different analyses are illustrated in Fig. S3.

Spatial risk patches

A total of nine spatial risk patches, which represent around 8% of the study area, were identified as suffering agricultural damage due to the ICP. The largest of these patches are Patch1 (approximately 23,500 km² with 49 damage records), Patch2 (about 8,600 km² with 13 damage records), and Patch3 (around 5,700 km² with 10 damage records), situated in the southwest, west, and northwest regions of the study area, respectively. Together, these three patches accounted for 80% of all predicted agricultural damage areas linked to the ICP within the study area (refer to Fig. 4; Table 3). Additionally, CAs covered roughly 8% of the predicted spatial risk patches.

Crop damage hotspots

Crop damage hotspots were mainly located in the western parts of the study area (Fig. 5). These hotspots were mainly concentrated in Patch1 and Patch2. The overlap between risk patches and hotspots was about 85%. The optimized hotspot analysis revealed that just 2.4% of these hotspot areas fell within the CAs.

Discussion

This research was carried out in southeastern Iran to forecast spatial risk patches for agriculture and crop damage attributed to the ICP. Our results revealed that the key factors influencing the spatial risk of agricultural damage from the ICP in the region were the distance to villages, orchards density, croplands density, and NDVI. The west regions exhibited the highest likelihood of human-ICP conflicts. We identified nine spatial risk patches for agricultural damage caused by the ICP, three of which accounted for approximately four-fifths of the total area of all identified risk patches. Furthermore, our results showed that the majority of high-risk damage areas (92%) were located outside the CAs.

Variables contribution

Previous studies have primarily focused on the habitat suitability of the ICP¹⁵, and its closely related species^{5,56,57}. Additionally, these studies have utilized land cover, climatic, and topographic variables to assess habitat suitability, often neglecting human-related factors such as villages and roads. Croplands have been identified as the most important variable influencing the habitat suitability of the crested porcupine in northern Italy⁵⁷. In addition, croplands and orchards were the second and fourth most important variables in the habitat suitability of the crested porcupine in Central Italy⁵, which aligns with our findings. However, in southern Italy, this species tends to inhabit forested areas in lower latitudes –where the species never been presence- more frequently due

| | Distance to villages | Distance to roads | Human population density | Croplands density | Orchards density | NDVI | Distance to CAs | BIO9 | BIO14 |
|--------------------|----------------------|-------------------|--------------------------|-------------------|------------------|------|-----------------|------|-------|
| Mean | 19.6 | 7.9 | 7.8 | 15.1 | 16.2 | 12.3 | 8.7 | 7.3 | 5.1 |
| Standard deviation | 1.9 | 1.1 | 2.2 | 2.5 | 2.3 | 1.4 | 2.1 | 1.3 | 1.1 |

Table 2. Average and standard deviation of variable contributions in the spatial risk assessment of agricultural damage inflicted by the Indian crested porcupine within the study area in southeastern Iran.

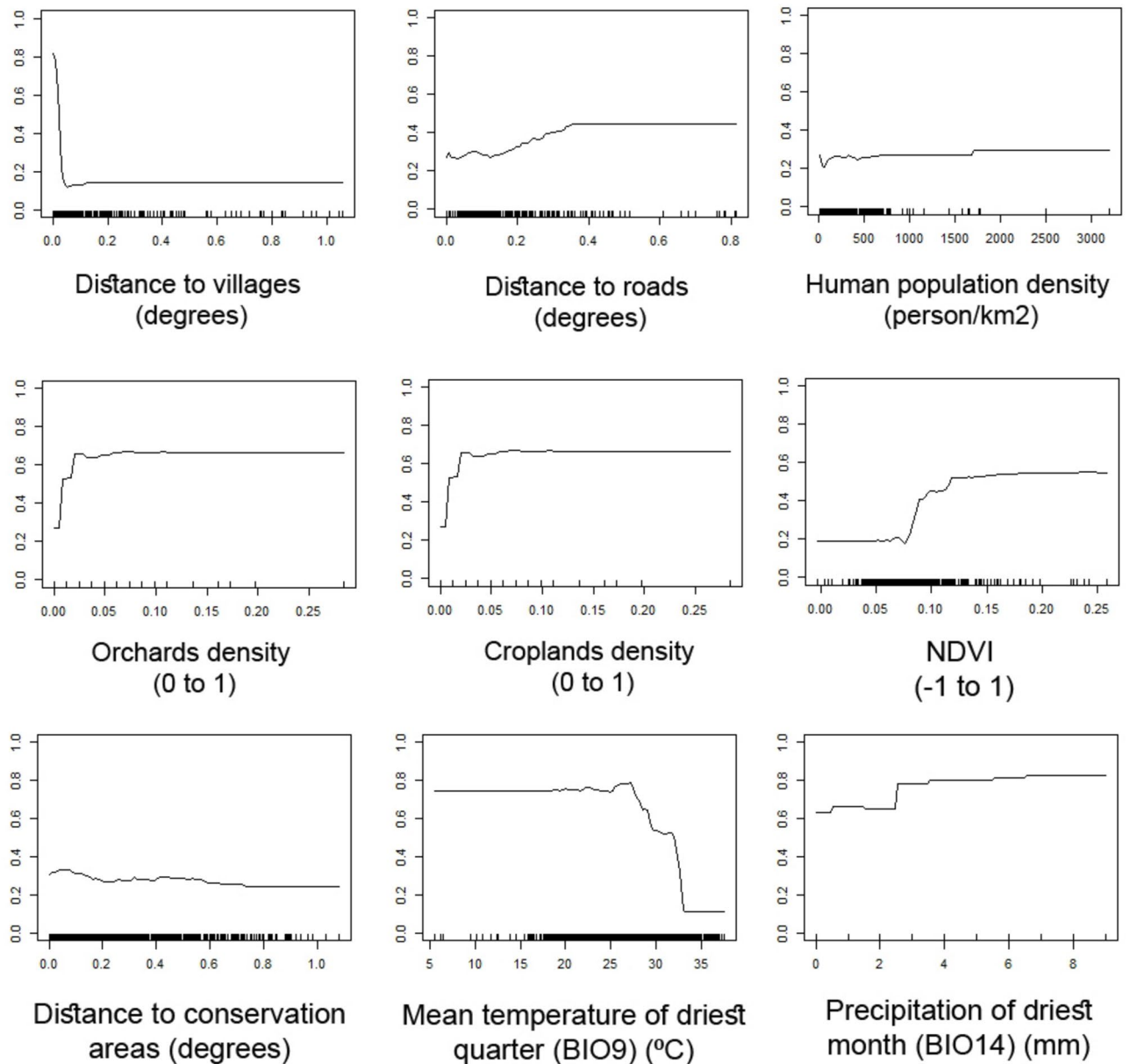


Fig. 2. Response curves depicting the agricultural damage attributed to the Indian crested porcupine in relation to environmental factors in the study area. The analysis employed the Generalized Boosted Model (GBM), recognized as the most precise model for this purpose. The Y-axis indicates the likelihood of agricultural damage caused by the Indian crested porcupine, with each degree representing approximately 11 km.

to climate change³⁹. Croplands were also identified as the second most important land cover type for the habitat suitability of the ICP in Iraq¹⁵. Since the orchards and croplands are situated near the villages, their proximity is considered the most significant factor for ICP in our study area. NDVI illustrates the trend of vegetation and indicates that the suitable range for the ICP includes woodlands in addition to orchards and croplands. The crested porcupine is also associated with forests and woodlands in both southern and northern Italy^{39,57}. Furthermore, NDVI has proven to be an important variable for assessing habitat suitability for the ICP in Iraq¹⁵.

Spatial risk patches and implication for mitigating conflicts

Previous research has indicated that the population of the ICP has increased in some areas while decreasing in others across southwestern Asia¹⁵. In regions experiencing population growth of the ICP and, consequently, greater damage to agricultural products, implementing a conservation program for the Persian leopard—its only natural predator—could be effective. Agricultural damage typically occurs during the warm season in farms and orchards, where various food sources are available for the ICP⁵⁷. Considering the significant role that the densities of orchards and croplands play in contributing to ICP conflict within the study area, farmers should

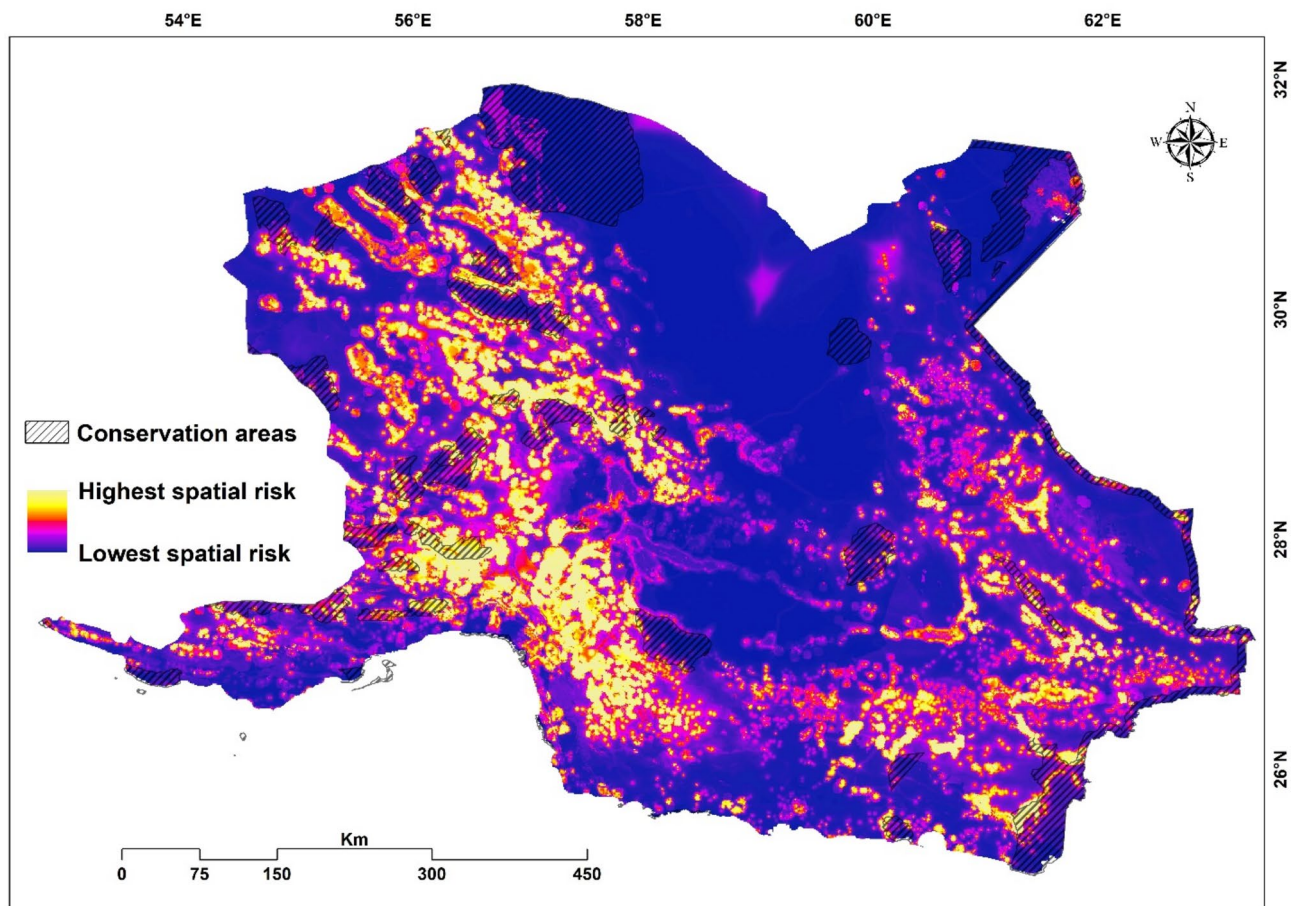


Fig. 3. Ensemble spatial risk model illustrating agricultural damage caused by the Indian crested porcupine in the study area based on five models of Generalized Linear Model (GLM), Multivariate Adaptive Regression Splines (MARS), Maximum Entropy (MaxEnt), Generalized Boosting Model (GBM), and Random Forest (RF). ArcGIS software version 10.1 (<https://www.esri.com/en-us/arcgis/products/arcgis-pro/resources>) was used to generate the figure.

implement measures to prevent ICPs from entering their fields and orchards, such as erecting fencing around their owned lands. Research indicates that, to date, there have been no reported conflicts between humans and porcupines in Rome. This may be attributed to the porcupines' strictly nocturnal behavior and the establishment of protective fencing around local agricultural areas, which likely facilitates coexistence between porcupines and humans⁵⁸. We found orchard density to be the second top variable contributing to ICP conflict in the study area, therefore we recommend installing thick fencing around each tree trunk or placing stones around the bases of trees can help prevent damage. In some regions of Pakistan, fences and dogs are employed to mitigate crop damage caused by ICPs⁵⁹.

Given the limited research on human-ICP conflict, we compared our findings with those related to a closely related species, the crested porcupine, in Italy, which represents a limitation of our study. Overall, the strategies recommended by Italians to mitigate conflict and deter porcupines from accessing orchards and agricultural lands, such as fencing, could also be applicable in Iran. This approach has also been proposed for the ICP in Pakistan, which shares similar ecological conditions with southeastern Iran. In addition, spatial risk modeling had some limitations due to scarcity of long-term monitoring data constrains predictive accuracy over time, incomplete geospatial records of conflict and reliance on simulated data rather than field observations in data-poor regions⁶⁰. Despite several limitations, spatial risk modeling has become a crucial tool for understanding and mitigating HWC.

In general, educating farmers about best practices for managing interactions with ICPs can empower them to implement effective strategies that reduce crop damage. Workshops and training sessions can teach farmers about crop protection methods and the biology of ICPs⁶¹. In addition, increasing local awareness about the benefits of ICPs in their area—such as the use of burrows by other animals as shelters and the role of burrows in retaining water for seeds—can be effective in preventing the decline of the ICP population due to human intervention^{15,62}.

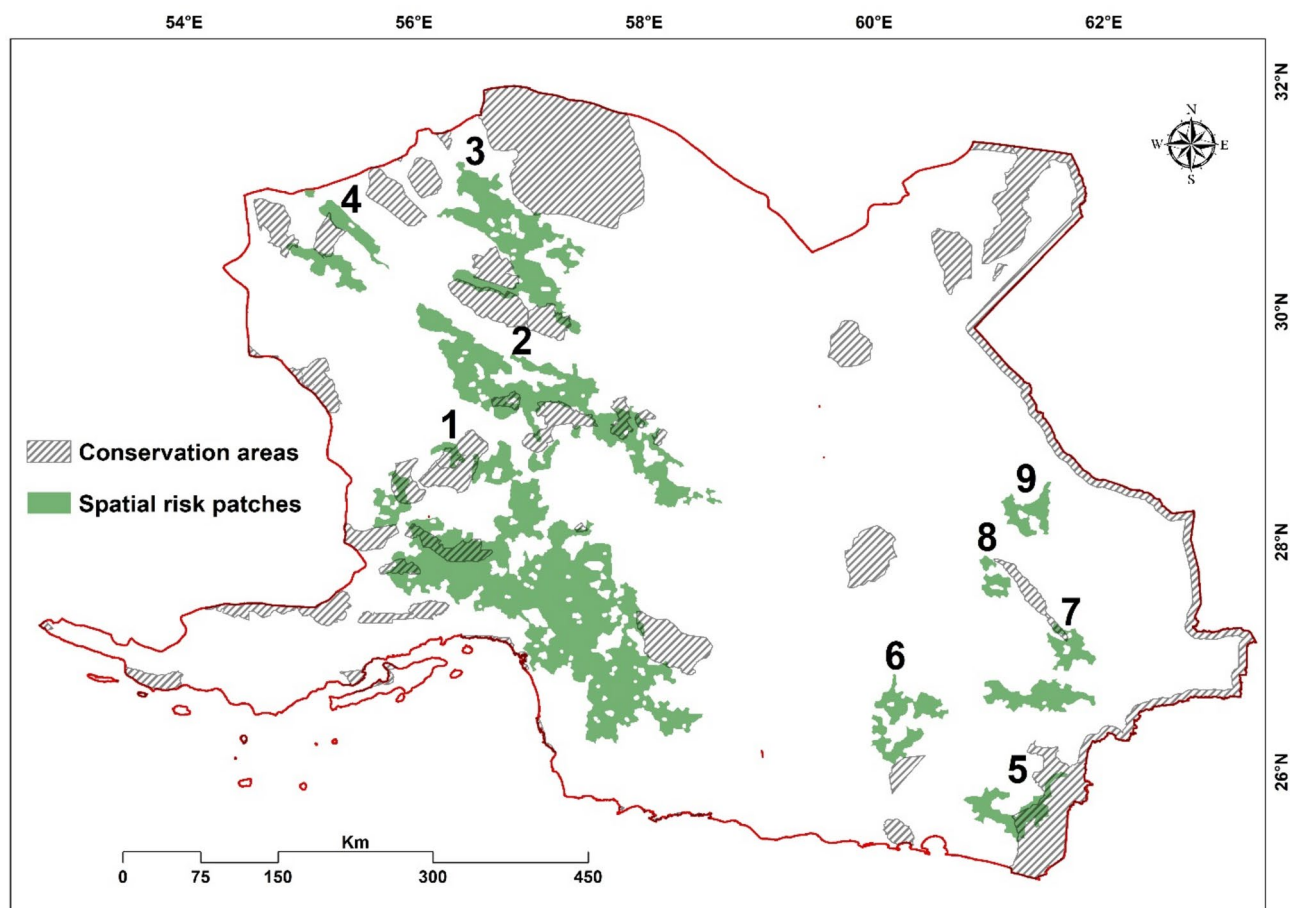


Fig. 4. Spatial risk patches for agricultural damage attributed to the Indian crested porcupine (Details regarding patch numbers can be found in Table 3). ArcGIS software version 10.1 (<https://www.esri.com/en-us/arcgis/products/arcgis-pro/resources>) was used to generate the figure.

| Patch number | Area (km ²) | Conservation areas within patches | | Conflicts records within patch |
|--------------|-------------------------|-----------------------------------|---------|--------------------------------|
| | | Area (km ²) | Percent | |
| 1 | 23556.52 | 1842.12 | 7.82 | 49 |
| 2 | 8579.49 | 752.185 | 8.77 | 13 |
| 3 | 5687.75 | 329.43 | 5.79 | 10 |
| 4 | 1905.94 | 83.82 | 4.39 | 9 |
| 5 | 1667.69 | 694.86 | 41.66 | 5 |
| 6 | 1865.44 | 0.35 | 0.02 | 7 |
| 7 | 2480.46 | 66.79 | 2.69 | 2 |
| 8 | 508.51 | 0 | 0 | 3 |
| 9 | 1011.25 | 0 | 0 | 3 |
| Total | 47263.05 | 3769.55 | 7.97 | 101 |

Table 3. Characteristics of the predicted Spatial risk areas for agricultural damage caused by the Indian crested Porcupine within the study area in southeastern Iran (Refer to Fig. 4 for patch numbers).

Conclusions

Anthropogenic factors and land cover were the primary contributors to agricultural damage caused by the ICP in the study area. Approximately 8% of the study area is classified as being at high risk for human-ICP conflict. Prompt action is necessary to tackle agricultural damage in the nine risk areas identified in this study, particularly in the three key patches located in the western region of the study area. These three patches represent four-fifths of all identified risk areas, and if budget limitations arise, conflict mitigation efforts can be concentrated on these

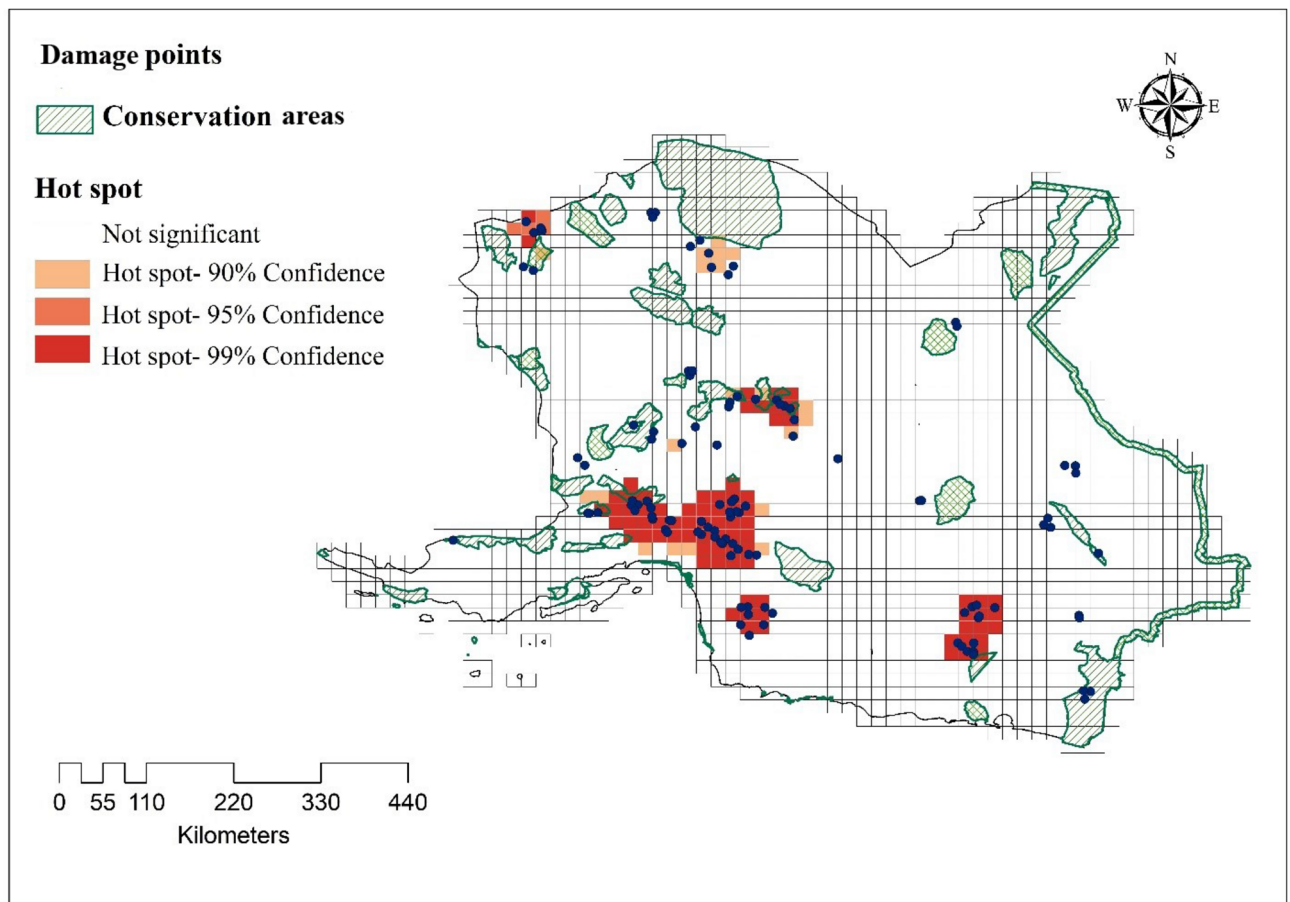


Fig. 5. Hotspots of crop damage caused by the Indian crested porcupine in southeastern Iran. The blue points indicate conflict records. Crop damage hotspots were illustrated by three confidence intervals of 90%, 95%, and 99%. The majority of these hotspots are situated in non-conservation areas. ArcGIS software version 10.1 (<https://www.esri.com/en-us/arcgis/products/arcgis-pro/resources>) was used to generate the figure.

three sites. To alleviate these conflicts, it is strongly recommended to implement fencing around private lands and enhance local knowledge.

Data availability

The datasets used and/or analyzed during the current study available from the corresponding author on reasonable request.

Received: 19 November 2024; Accepted: 25 April 2025

Published online: 02 May 2025

References

- Woodroffe, R., Thirgood, S., Spampns Rabinowitz, A. The impact of human-wildlife conflict on natural systems. *People Wildl.* 1–12. <https://doi.org/10.1017/CBO9780511614774.002> (2005).
- Mpakairi, K., Ndaimani, H., Vingi, K., Madiri, T. H. & Nekatambe, T. Ensemble modelling predicts human carnivore conflict for a community adjacent to a protected area in Zimbabwe. *Afr. J. Ecol.* **56**, 957–963 (2018).
- Mackenzie, C. A. & Ahabyona, P. Elephants in the garden: financial and social costs of crop raiding. *Ecol. Econ.* **75**, 72–82 (2012).
- Ji, Y., Wei, X., Liu, F., Li, D. & Li, J. Spatial-temporal patterns of human-wildlife conflicts under coupled impact of natural and anthropogenic factors in Mt. Gaoligong, Western Yunnan, China. *Glob. Ecol. Conserv.* **40**, e02329 (2022).
- Franchini, M. et al. Get out from my field! The role of agricultural crops in shaping the habitat selection by and suitability for the crested Porcupine in Central Italy. *Mamm. Res.* **69**, 411–421 (2024).
- Almasieh, K., Zamani, N. & Piri, R. An ensemble modeling approach to predict spatial risk patches of the Persian leopard-livestock conflicts in Lorestan Province, Iran. *Environ. Sci. Pollut. Res.* **30**, 93002–93013 (2023).
- Anand, S. & Radhakrishna, S. Investigating trends in human-wildlife conflict: is conflict escalation real or imagined? *J. Asia-Pac. Biodivers.* **10**, 154–161 (2017).
- Mohammadi, A., Alambeigi, A., López-Bao, J. V., Taghavi, L. & Kaboli, M. Living with wolves: lessons learned from Iran. *Conserv. Sci. Pract.* **4**, e12667 (2022).
- Kaartinen, S., Luoto, M. & Kojola, I. Carnivore-livestock conflicts: determinants of Wolf (*Canis lupus*) depredation on sheep farms in Finland. *Biodivers. Conserv.* **18**, 3503–3517 (2009).

10. Khorozyan, I., Ghoddousi, S., Soufi, M., Soofi, M. & Waltert, M. Cattle selectivity by leopards suggests ways to mitigate human–leopard conflict. *Ecol. Evol.* **8**, 8011–8018 (2018).
11. Dai, Y. et al. Human-carnivore conflicts and mitigation options in Qinghai Province, China. *J. Nat. Conserv.* **53**, 125776 (2020).
12. Davoli, M. et al. Changing patterns of conflict between humans, carnivores and crop-raiding prey as large carnivores recolonize human-dominated landscapes. *Biol. Conserv.* **269**, 109553 (2022).
13. Nyhus, P. J. Human-wildlife conflict and coexistence. *Annu. Rev. Environ. Resour.* **41**, 143–171 (2016).
14. *Hystrix indica*: Amori, G., Hutterer, R., Kryštufek, B., Yigit, N., Mitsainas, G. & Palomo, L. IUCN Red List of Threatened Species (2016). <https://doi.org/10.2305/IUCN.UK.2021-1.RLTS.T10751A197516522.EN>
15. Nolan, V., Kaky, E. D., Alatawi, A. S. & Gilbert, F. Mapping the Indian crested Porcupine across Iraq: the benefits of species distribution modelling when species data are scarce. *Mamm. Biol.* **102**, 1851–1866 (2022).
16. National Red data book of mammals in Jordan-resource | IUCN. <https://iucn.org/resources/grey-literature/national-red-data-book-mammals-jordan>
17. Bilimliri, Y., Doç Gökhan YÜRÜMEZ Batman Üniversitesi Fen Edb Fak Biyoloji Bölümü, Y., Doç Servet ULUTÜRK Batman Üniversitesi, Y. & Edb Fak Biyoloji Bölümü, F. Batman Üniversitesi Batman University Distribution of Indian Crested Porcupine *Hystrix indica* (Kerr, 1792) (Mammalia: Rodentia) in Batman Province. *J. Life Sci.* **1** (2016).
18. Ziaie, H. A Field Guide to The Mammals of Iran. 1th Edition, Iran Wildlife Center, Tehran. References - Scientific Research Publishing (2008). <https://www.scirp.org/reference/referencespapers?referenceid=1757158>
19. Determinants of occupancy and burrow site selection by Indian crested porcupine in Keoladeo National Park, Bharatpur, Rajasthan, India on JSTOR. <https://www.jstor.org/stable/26163993>
20. Hafeez, S., Ashfaq, M., Khan, G. S. & Khan, Z. H. Damage inflicted by the Indian crested Porcupine, *Hystrix indica*, on forestry and agricultural systems in Punjab, Pakistan. *J. Asian Afr. Stud.* **47**, 168–175 (2012).
21. Ashraf, R. Z. et al. Evaluation of economic loss caused by Indian crested Porcupine (*Hystrix indica*) in agricultural land of district Muzaffarabad, Azad Jammu and Kashmir, Pakistan. *Braz. J. Biol.* **83**, 1–12 (2023).
22. Wilson, D. E., Lacher, T. E. & Mittermeier, R. A. Handbook of the mammals of the world. 6. Lagomorphs and rodents I. 987 (2016).
23. Ehtisham et al. Identification and crop damage assessment of Indian crested porcupine (*Hystrix indica*) in selected zones of Abbottabad, Pakistan. *Braz. J. Biol.* **82**, 1–10 (2022).
24. Yusefi, G. H., Faizolahi, K., Darvish, J., Safi, K. & Brito, J. C. The species diversity, distribution, and conservation status of the terrestrial mammals of Iran. *J. Mamm.* **100**, 55–71 (2019).
25. Karami, M., Ghadirian, T. & Faizolahi, K. *The Atlas of Mammals of Iran; Jahad Daneshgahi, Kharazmi Branch* (Department of the Environment of Iran, 2016).
26. Mori, E., Molteni, R., Ancillotto, L., Ficetola, G. F. & Falaschi, M. Spatial ecology of crested porcupine in a metropolitan landscape. *Urban Ecosyst.* **25**, 1797–1803 (2022).
27. Mawere, K. K. et al. Application of maximum entropy (MaxEnt) to understand the spatial dimension of human–wildlife conflict (HWC) risk in areas adjacent to Gonarezhou National Park of Zimbabwe. *Ecol. Soc.* <https://doi.org/10.5751/ES-14420-280318> (2023).
28. Behdarvand, N. et al. Spatial risk model and mitigation implications for wolf–human conflict in a highly modified agroecosystem in Western Iran. *Biol. Conserv.* **177**, 156–164 (2014).
29. Miller, J. R. B. Mapping attack hotspots to mitigate human–carnivore conflict: approaches and applications of spatial predation risk modeling. *Biodivers. Conserv.* **24**, 2887–2911 (2015).
30. Hipólito, D. et al. Brown bear damage: patterns and hotspots in Croatia. *Oryx* **54**, 511–519 (2020).
31. Eshtiahi, A., Naderi, S., Mohammadi, A. & Wan, H. Y. Identifying wild Boar (*Sus scrofa*) crop damage hotspots to mitigate human-wild Boar conflicts in Northern Iran. *Glob. Ecol. Conserv.* **54**, e03065 (2024).
32. Nair, R. P. & Jayson, E. A. Occurrence of the Indian crested porcupine (*Hystrix indica* Kerr.1792) and the damage on plantation crops in the Nilambur forest divisions of Southern Western Ghats, Kerala, India. *Agric. Sci. Dig.* **39**, 301–305 (2019).
33. Khattak, R. H. et al. Understanding the dynamics of human–wildlife conflicts in north-western Pakistan: implications for sustainable conservation. *Sustainability* **13**, 10793 (2021).
34. Almasieh, K., Kaboli, M. & Beier, P. Identifying habitat cores and corridors for the Iranian black bear in Iran. *Ursus* **27**, 18–30 (2016).
35. Brown, J. L. SDMtoolbox: A python-based GIS toolkit for landscape genetic, biogeographic and species distribution model analyses. *Methods Ecol. Evol.* **5**, 694–700 (2014).
36. Venter, O. et al. Global terrestrial human footprint maps for 1993 and 2009. *Sci. Data* **3**, 1–10 (2016).
37. Sanderson, E. W. et al. The human footprint and the last of the wild. *BiSci* **52**, 891 (2002).
38. Almasieh, K., Rouhi, H. & Hasti, F. Identifying core habitats and connectivity paths for the conservation of mouflon (*Ovis gmelini*) in Western Iran. *Glob. Ecol. Conserv.* **41**, e02377 (2023).
39. Mori, E. et al. How the south was won: current and potential range expansion of the crested porcupine in Southern Italy. *Mamm. Biol.* **101**, 11–19 (2021).
40. Fick, S. E. & Hijmans, R. J. WorldClim 2: new 1-km spatial resolution climate surfaces for global land areas. *Int. J. Climatol.* **37**, 4302–4315 (2017).
41. Esri. ArcGIS 10.1. *Environ. Syst. Res. Institute, Redlands, CA, USA* (2012).
42. Jueterbock, A. 'MaxentVariableSelection' vignette (2015).
43. Team, R. C. R. *A Language and Environment for Statistical Computing* (R Foundation for Statistical Computing, 2019).
44. Zuur, A. F., Ieno, E. N. & Elphick, C. S. A protocol for data exploration to avoid common statistical problems. *Methods Ecol. Evol.* **1**, 3–14 (2010).
45. Naimi, B., Hamm, N. A. S., Groen, T. A., Skidmore, A. K. & Toxopeus, A. G. Where is positional uncertainty a problem for species distribution modelling? *Ecography (Cop.)* **37**, 191–203 (2014).
46. Thuiller, W., Lafourcade, B., Engler, R. & Araújo, M. B. BIOMOD—A platform for ensemble forecasting of species distributions. *Ecography (Cop.)* **32**, 369–373 (2009).
47. Araújo, M. B. & New, M. Ensemble forecasting of species distributions. *Trends Ecol. Evol.* **22**, 42–47 (2007).
48. Almasieh, K. & Mohammadi, A. Assessing landscape suitability and connectivity for effective conservation of two semi-desert ungulates in Iran. *Conserv. Sci. Pract.* **5**, e13047 (2023).
49. Ashrafzadeh, M. R., Naghipour, A. A., Haidarian, M. & Khorozyan, I. Modeling the response of an endangered flagship predator to climate change in Iran. *Mamm. Res.* **64**, 39–51 (2019).
50. Rezaei, S., Mohammadi, A., Shadloo, S., Ranaie, M. & Wan, H. Y. Climate change induces habitat shifts and overlaps among carnivores in an arid and semi-arid ecosystem. *Ecol. Inf.* **77**, 102247 (2023).
51. ESKILDSEN, A. et al. Testing species distribution models across space and time: high latitude butterflies and recent warming. *Glob. Ecol. Biogeogr.* **22**, 1293–1303 (2013).
52. Mohammadi, A., Almasieh, K. & Vaissi, S. Ungulates conservation in the face of human development: mining and roads' influences on habitat and connectivity in Iran's central plateau. *Ecol. Inf.* **81**, 102656 (2024).
53. Barbet-Massin, M., Jiguet, F., Albert, C. H. & Thuiller, W. Selecting pseudo-absences for species distribution models: how, where and how many? *Methods Ecol. Evol.* **3**, 327–338 (2012).
54. Calambás-Trochez, L. F. et al. Climate and land-use changes coupled with low coverage of protected areas threaten palm species in South Brazilian grasslands. *Perspect. Ecol. Conserv.* **19**, 345–353 (2021).

55. Ahmadi, M. et al. Species and space: a combined gap analysis to guide management planning of conservation areas. *Landsch. Ecol.* **35**, 1505–1517 (2020).
56. Mori, E., Sforzi, A. & Di Febbraro, M. From the apennines to the Alps: recent range expansion of the crested porcupine *Hystrix cristata* L., 1758 (Mammalia: Rodentia: Hystricidae) in Italy. *Ital. J. Zool.* **80**, 469–480 (2013).
57. Torretta, E., Orioli, V., Bani, L., Mantovani, S. & Dondina, O. En route to the north: modelling crested porcupine habitat suitability and dispersal flows across a highly anthropized area in Northern Italy. *Mamm. Biol.* **101**, 1067–1077 (2021).
58. Lovari, S., Corsini, M. T., Guazzini, B., Romeo, G. & Mori, E. Suburban ecology of the crested porcupine in a heavily poached area: a global approach. *Eur. J. Wildl. Res.* **63**, 1–10 (2017).
59. Safeer, B., Rasheed, Z., Altaf, M., Manzoor, I. & Yasrub, S. Assessment of human-Indian crested porcupine (*Hystrix indica*) conflict in district Bagh. *Azad Jammu Kashmir J. Wildl. Ecol.* **2**, 1–12 (2018).
60. Wu, Q., Dai, Y. & Sun, Q. Human-wildlife conflict patterns and hotspot prediction in the southern foothills of the Daba mountains, China. *Front. Ecol. Evol.* **12**, 1435811 (2024).
61. Redpath, S. M. et al. Understanding and managing conservation conflicts. *Trends Ecol. Evol.* **28**, 100–109 (2013).
62. Khan, A. A., Ahmad, S., Hussain, I. & Munir, S. Deterioration impact of Indian crested porcupine, *Hystrix indica*, on forestry and agricultural systems in Pakistan. *Int. Biodeterior. Biodegrad.* **45**, 143–149 (2000).

Acknowledgements

We would like to express our gratitude to the rangers and experts from the three provincial offices of the Department of Environment of Iran for providing the conflict records used in this study. We would like to thank the editor and anonymous reviewers for their valuable feedback and constructive comments that greatly improved this manuscript.

Author contributions

K.A. conceptualized and designed the project. K.A. collected the data. K.A. and A.M analyzed the data and interpreted results. K.A. and A.M wrote the manuscript. K.A. and A.M authors discussed the results and commented on the manuscript.

Declarations

Competing interests

The authors declare no competing interests.

Ethical approval

The methodology for this study received approval from the Ethics Committee of the Agricultural Sciences and Natural Resources University of Khuzestan (Ethics Approval Number: 1403-08). All methods were conducted in accordance with the relevant guidelines and regulations.

Additional information

Supplementary Information The online version contains supplementary material available at <https://doi.org/10.1038/s41598-025-00232-x>.

Correspondence and requests for materials should be addressed to K.A.

Reprints and permissions information is available at www.nature.com/reprints.

Publisher's note Springer Nature remains neutral with regard to jurisdictional claims in published maps and institutional affiliations.

Open Access This article is licensed under a Creative Commons Attribution-NonCommercial-NoDerivatives 4.0 International License, which permits any non-commercial use, sharing, distribution and reproduction in any medium or format, as long as you give appropriate credit to the original author(s) and the source, provide a link to the Creative Commons licence, and indicate if you modified the licensed material. You do not have permission under this licence to share adapted material derived from this article or parts of it. The images or other third party material in this article are included in the article's Creative Commons licence, unless indicated otherwise in a credit line to the material. If material is not included in the article's Creative Commons licence and your intended use is not permitted by statutory regulation or exceeds the permitted use, you will need to obtain permission directly from the copyright holder. To view a copy of this licence, visit <http://creativecommons.org/licenses/by-nc-nd/4.0/>.

© The Author(s) 2025